Supplementary Figure 1

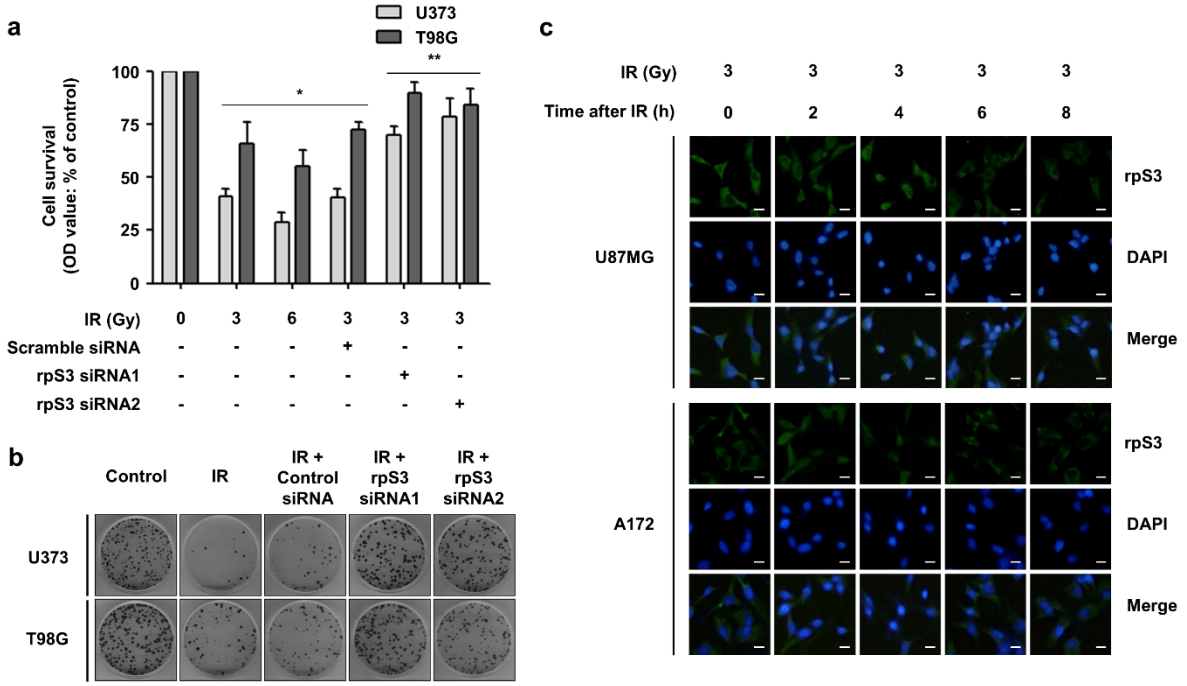

Supplementary Figure S1 Knockdown of rpS3 enhances the resistance of GBM cells to irradiation. (**a**) Short-term effects of rpS3 knockdown on cell growth in other GBM cell lines, U373 and T98G cells, following radiation exposure were assessed with an MTT assay. $^{*}p<0.05$ vs. non-irradiated cells, $^{**}p<0.05$ vs. irradiated cells treated with/without scramble siRNA. (**b**) Long-term effects of rpS3 knockdown on cell growth in U373 and T98G cells following radiation exposure were assessed with a colony forming assay. (**c**) Radiation-induced translocation of rpS3 from the cytoplasm to the nucleus in a time-dependent manner (0, 2, 4, 6, and 8 h) was assessed by IF staining. Scale bars, 25μm.

Supplementary Figure 2

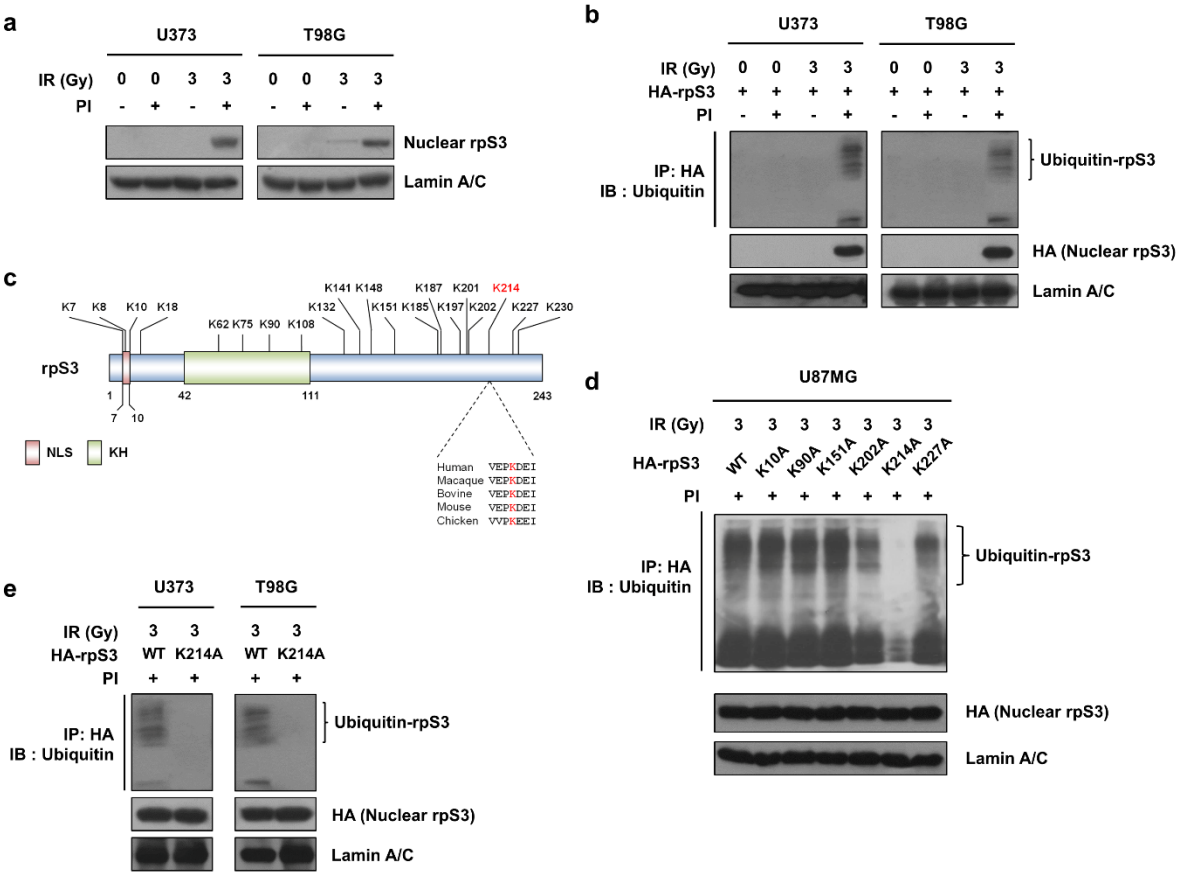

Supplementary Figure S2 Poly-ubiquitination is required for degradation of rpS3 in irradiated GBM cells. (**a**) The effects of proteasome inhibition on the protein stability of nuclear rpS3 in U373 and T98 cells were measured by Western blotting. (**b**) The accumulation of poly-ubiquitinated nuclear rpS3 in response to radiation was measured. U373 and T98G cells expressing HA-rpS3 were treated with or without PI. (**c**) Schematic presentation for 20 Lys residues of rpS3, which are targets for ubiquitination. (**d**) The identification of specific Lys residues on the poly-ubiquitination of rpS3 in response to irradiation was measured using six rpS3 mutants (K10A, K90A, K151A, K202A, K214A, or K227A). (**e**) The effects of Lys214 residue on the poly-ubiquitination of rpS3 were measured. U373 and T98G cells expressing rpS3 WT or K214A were treated with PI.

Supplementary Figure 3

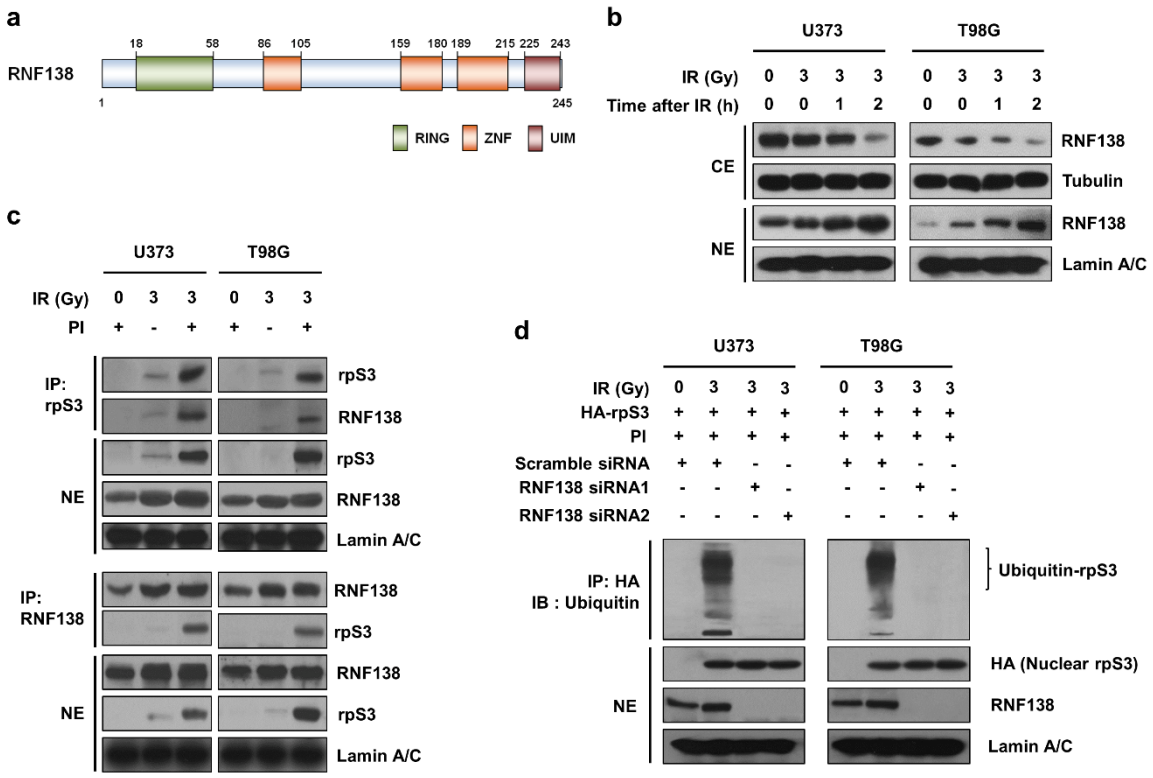

Supplementary Figure S3 RpS3 is ubiquitinated by RNF138 in response to radiation. (**a**) Schematic presentation for motifs and domains of RNF138 consisting of RING domain, ZNF motifs, and UIM domain. (**b**) Radiation-induced translocation of RNF138 from the cytoplasm to the nucleus of U373 and T98G cells was assessed by Western blotting after cytoplasmic or nuclear fractionation. (**c**) RpS3-RNF138 interaction in the nucleus of U373 and T98G cells after treatment of PI and irradiation was monitored by a reciprocal IP assay. (**d**) The effects of RNF138 knockdown on the ubiquitination of rpS3 in U373 and T98G cells were measured.

Supplementary Figure 4

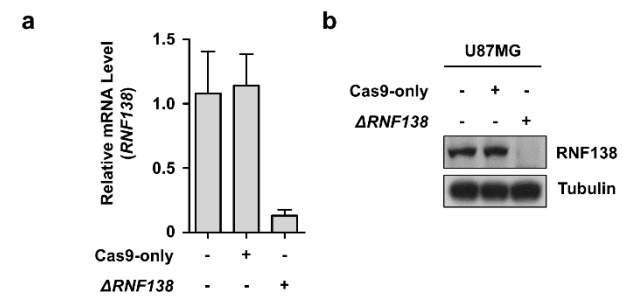

Supplementary Figure S4 The knockdown efficacy of RNF138 in Δ*RNF138* U87MG cells was verified. (**a**) U87MG cells were treated with inactive control gRNA/Cas9 (Cas9-only) or RNF138-targeting gRNA/Cas9 (Δ*RNF138*). The mRNA levels of *RNF138* were measured to confirm the knockdown efficacy of RNF138 in Δ*RNF138* U87MG cells generated by the CRISPR/Cas9 system. (**b**) The protein levels of RNF138 were measured to confirm the knockdown efficacy of RNF138 in Δ*RNF138* U87MG cells generated by the CRISPR/Cas9 system.

Supplementary Figure 5

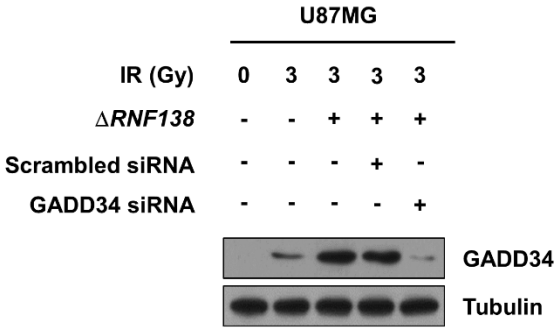

Supplementary Figure S5 The knockdown efficacy of GADD34 siRNA in Δ*RNF138* U87MG cells was verified by Western blotting.

Supplementary Figure 6

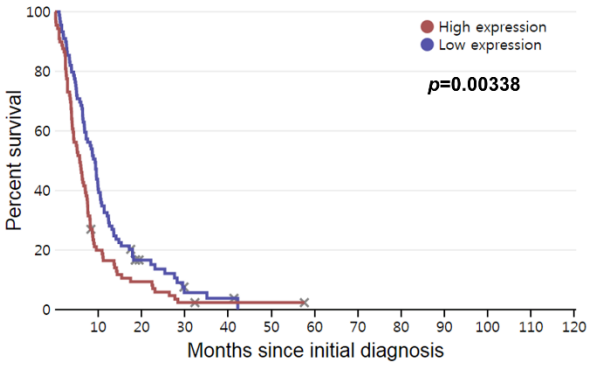

Supplementary Figure S6 The prognostic value of RNF138 in GBM patients obtained from Betastasis database. It indicated that RNF138-positive (high levels) patients showed poor prognosis than RNF138-negative (low levels) patients (*p*-value = 0.00338).